

FIRST RESULTS FROM GODDARD HIGH-RESOLUTION SPECTROGRAPH: C I, S I, AND CO TOWARD ζ PERSEI AND THE PHYSICAL CONDITIONS IN DIFFUSE CLOUDS

ANDREW M. SMITH,¹ FREDERICK C. BRUHWEILER,² DAVID L. LAMBERT,³ BLAIR D. SAVAGE,⁴
 JASON A. CARDELLI,⁴ DENNIS C. EBBETS,⁵ CHENG-HSIUAN LYU,⁶ AND YARON SHEFFER³

Received 1991 April 1; accepted 1991 May 23

ABSTRACT

Observations made by the Goddard High Resolution Spectrograph of the cool, neutral interstellar gas in the line of sight to ζ Per are reported. Heliocentric velocities and equivalent widths were measured for absorption lines of C I and S I. Synthetic spectra were computed and fitted to the observed CO (2–0) and (3–0) bands in the $A^1\Pi-X^1\Sigma^+$ system. Derived populations of the C I ground-state fine-structure levels and the CO ground-state rotational levels were used to derive densities of two of the three, and possibly four, detected cloud components. The velocity component displaying the strongest C I absorption reveals extraordinarily high pressure ($P/k > 4.3 \times 10^4 \text{ cm}^{-3} \text{ K}$).

Subject headings: interstellar: matter — interstellar: molecules — ultraviolet: spectra

1. INTRODUCTION

In this letter we present the first observational results from the Goddard High Resolution Spectrograph (GHRS) of neutral and molecular species that represent diagnostics of the physical conditions in the interiors of diffuse interstellar clouds. Specifically, we present results at a resolution of $\sim 3.7 \text{ km s}^{-1}$ for the observed species of C I, S I, and CO, seen in the UV spectrum of ζ Per, an O9 III star in the Per OB2 association located at a distance of $\sim 400 \text{ pc}$. The results reported here complement those of Savage et al. (1991) and Cardelli et al. (1991) concerning the interstellar ionic species in the same line of sight.

2. OBSERVATIONS AND DATA REDUCTION

The data acquisition is described by Savage et al. (1991) and Cardelli et al. (1991). In this work the data pertain to echelle spectra obtained through the 0'25 square small science aperture (SSA) at six wavelength settings of the GHRS echelle using the D1 detector. Each spectrum was obtained using the standard FP-SPLIT option, which splits each exposure into four subexposures acquired at slightly different carousel settings. For some of the data, the actual count rate was lower than that anticipated due to both improper centering in the small aperture and to spacecraft "jitter" of amplitude larger than the size of the SSA; resulting signal-to-noise ratios were typically 20–25. Excepting the 1191 Å region, standard procedures were used for subtracting background and echelle scattered light contributions from the echelle data (see Cardelli et al. 1991; Savage et al. 1991). The cores of the saturated interstellar lines in Si II at 1190 and 1193 Å were used to establish a zero flux level in the 1191 Å region. The resultant net spectrum is presented in Figure 1.

After the net spectrum in each wavelength region was obtained, normalized spectra were produced by dividing the net spectrum by a cubic spline fit to the stellar continuum and rotationally broadened stellar features. All equivalent-width measurements and spectral profile fitting were accomplished using these normalized spectra.

3. THE INTERSTELLAR LINE SPECTRUM

The measured equivalent widths for the detected features of C I and S I with their formal errors are given in Table 1. These have been determined by fitting multiple Gaussian profiles to the normalized spectra of each of the studied species (see Fig. 2). Each Gaussian profile corresponded to a velocity component along the line of sight; component velocities which were approximately the same were forced to be equal. Derived velocities are absolute heliocentric values after corrections have been applied following Cardelli et al. (1991). The relative internal velocity scale should be accurate to $\sigma \approx 0.5 \text{ km s}^{-1}$. The errors denote $\pm \sigma$ as determined from Poisson statistics, errors that arise from choice of continuum levels, and uncertainties in corrections for scattered light and background.

The derivation of atomic column densities was carried out by two methods; first, the curve-of-growth procedure in which the derived equivalent widths given in Table 1 were used, and second, the inverse optical depth method of Savage & Sembach (1991). The second approach served as a check on the curve-of-growth method and placed strong constraints on the column densities of the observed species. The two methods produce similar results. The curve-of-growth results for the 6 and 10 km s^{-1} components are given in Table 2. These results are based upon an allowed range of the velocity dispersion parameter, b , between 0.9 and 2.0 km s^{-1} . The inverse optical depth method yields total logarithmic column densities of 14.50 ± 0.09 , 14.40 ± 0.09 , 13.84 ± 0.08 , and 13.02 ± 0.12 for C I, C I*, C I**, and S I, respectively. Atomic data from the compilation of Morton (1991) were used.

3.1. Interstellar C I

The higher velocity resolution of the GHRS lets us distinguish among at least three absorbing components. Figure 2 clearly shows that the C I (3P_2) atoms are found in only the 6.0

¹ NASA/Goddard Space Flight Center, Code 681, Greenbelt, MD 20771.
² Catholic University of America/CSC, Physics Department, Washington, DC 20064.
³ University of Texas at Austin, Astronomy Department, Austin, TX 78712.
⁴ University of Wisconsin-Madison, Astronomy Department, 475 North Charter Street, Madison, WI 53706.
⁵ Ball Aerospace Systems Division, Box 1062, JWF-3, Boulder, CO 80306.
⁶ Catholic University of America, Physics Department, Washington, DC 20064.

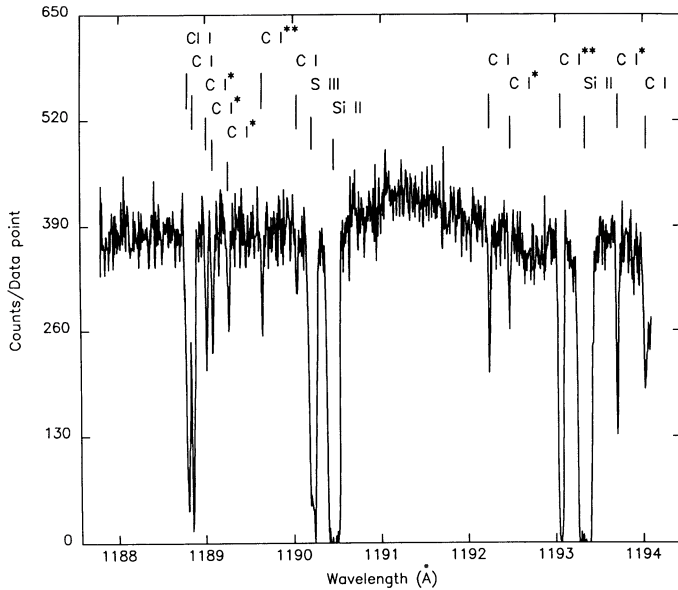


FIG. 1.—Echelle data for ξ Per from 1188 to 1194 Å: Leader lines mark transitions in C I, C I*, C I**, C I, S III, and Si II, as listed in Table 1. Weakest feature, C I λ 1190.02, has equivalent width = 4.8 mÅ, representing 2σ detection.

km s⁻¹ component, C I (³P₁) atoms are found in the 6.0 and 10.0 km s⁻¹, and the ground-state C I (³P₀) atoms are found in the three components 6.0, 10.0, and 13.2 km s⁻¹. [There is a suggestion of absorption by C I (³P₀) at 3.5 km s⁻¹.] The equivalent widths of these lines are in good agreement with those measured by Jenkins & Shaya (1979) (see Table 1).

The derived C I column densities for the three fine-structure levels toward ξ Per are also presented in Table 2. The quoted

TABLE 1
IDENTIFIED C I AND S I FEATURES IN ξ PERSEI

Species	Lab λ	f_{ij}	Equivalent Widths ^a (mÅ)				Formal errors
			3.5	6.0	10.0	13.2	
C I	1188.8332	1.68E-2	2.5?	18.7	9.6	4.8	± 1.9
	1190.0208	3.80E-3 ^b		4.8			± 2.3
	1192.2175	2.63E-3		6.9	4.1		± 2.2
	1193.9955	9.41E-3 ^b		8.9	7.1		± 2.2
	1280.1353	2.43E-2	4.4?	18.3	12.8	10.1	± 1.9
C I*	1188.9926	5.59E-3		10.1	1.8		± 2.2
	1189.0649	4.19E-3		10.1			± 2.1
	1189.2487	6.98E-3 ^b		8.9			± 2.2
	1192.4507	2.10E-3		6.4	1.3		± 2.3
	1193.6787	3.92E-3 ^b		10.7	7.1		± 2.2
	1279.0558	1.78E-3		7.9			± 1.9
	1279.8904	1.37E-2		17.7	5.5		± 1.9
	1280.4042	4.38E-3		11.5			± 1.9
	1280.5970	6.84E-3		13.6	3.6		± 2.0
C I**	1189.6307	1.26E-2		8.9			± 2.1
	1277.7229	1.45E-2		9.7			± 1.6
	1280.3328	1.47E-2		10.4	2.7?		± 2.0
	1280.8470	5.41E-3		6.0	1.4?		± 2.1
S I	1303.4300	2.91E-2	3.9 ^c				± 2.0
	1473.9943	7.30E-2		10.1	1.3		± 2.1
	1474.3785	1.63E-2 ^b	3.0?	2.2			± 2.0
	1807.3113	1.11E-1	7.7?	15.4	3.1		± 0.9

^a Equivalent widths are given for four velocity components (km s⁻¹). The approximate detection limit is 2.2 mÅ.

^b Oscillator strength (f_{ij}) incorrect?

^c Total equivalent width.

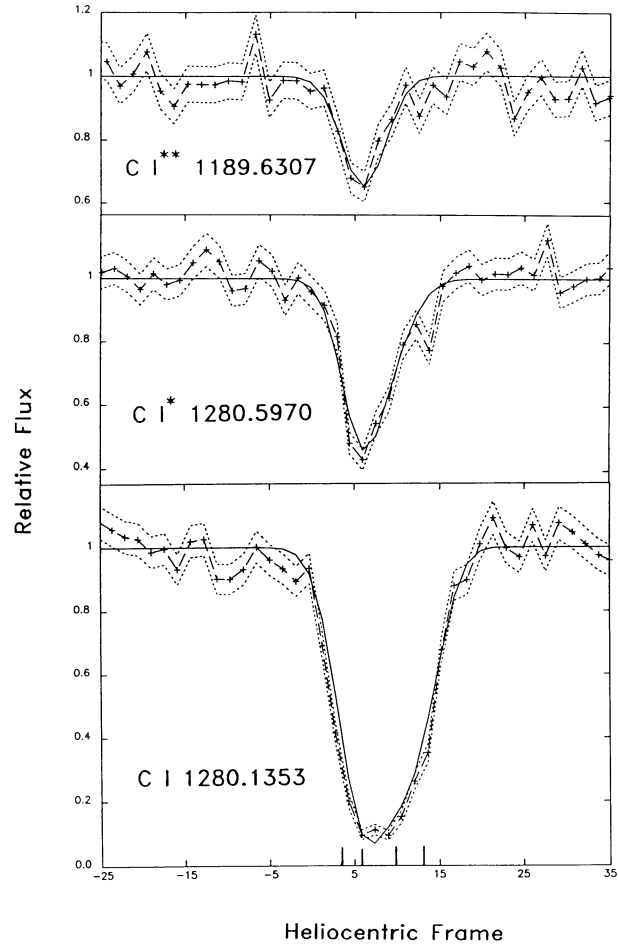


FIG. 2.—Normalized C I spectra showing transitions from ground-state, ³P₀, and from elevated fine-structure levels, ³P₁ and ³P₂. Crosses: observations. Dashed lines: $\pm 1\sigma$ counting statistics uncertainty. Solid lines: sum of Gaussian profiles using contributions from each cloud component with velocities indicated by short vertical lines.

errors reflect the combined errors of fit to the curve of growth and those of the derived equivalent widths, and possible errors in the oscillator strengths. There are additional effects which come about from partitioning absorption among the differing velocity components. We have attempted to constrain the pressure of the gas in which the atomic carbon is located by using the analysis of Jenkins & Shaya (1979), who predicted the relative population ratios, C I**/C I(total) and C I*/C I(total), for a range of temperatures and densities with a general interstellar radiation field and a radiation field 10 times larger. Our derived abundance ratios are $0.37 < C I^*/C I(\text{total}) < 0.50$ and $0.11 < C I^{**}/C I(\text{total}) < 0.19$ for the 6.0 km s⁻¹ component, and $0.17 < C I^*/C I(\text{total}) < 0.26$ and $C I^{**}/C I(\text{total}) < 0.10$

TABLE 2
LOGARITHMS OF COLUMN DENSITIES

Species	6 km s ⁻¹		10 km s ⁻¹	
	lower limits	upper limits	lower limits	upper limits
C I	14.36	14.50	14.07	14.22
C I*	14.36	14.58	13.58	13.67
C I**	13.83	14.16	13.22	13.26
Total	14.72	14.93	14.23	14.36
S I	12.86	12.98	NA	NA

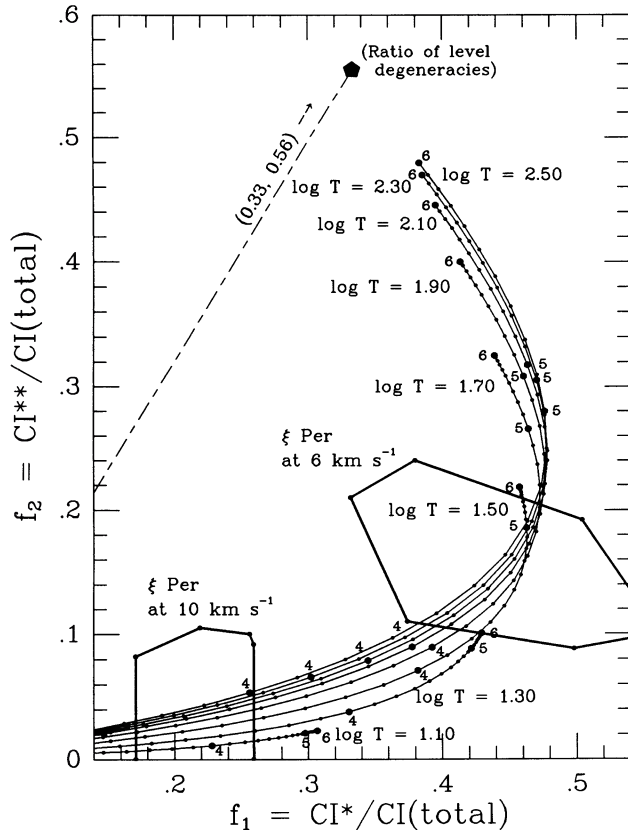


FIG. 3.—Domains for the population ratios of C I column densities superposed on Fig. 6a of Jenkins & Shaya (1979). *Solid lines*: computed population ratios for carbon atoms in excited fine-structure levels, 3P_1 and 3P_2 , for various gas temperatures. Pressures are indicated by tick marks on curves at 0.1 dex in P/k . Filled circles represent integer values of $\log P/k$. Computations include optical pumping from a general radiation field.

for the 10.0 km s^{-1} component. The domains defined by these uncertainties have been plotted on a Jenkins and Shaya diagram, as shown in Figure 3.

Of the three, possibly four, components identified toward ξ Per, two are at moderate to high density. The highest column density component at 6.0 km s^{-1} also appears to be at the highest pressure, with an implied $\log(P/k) \geq 4.3$ for $T = 32 \text{ K}$. The component at 10 km s^{-1} has a pressure roughly a factor of 10 lower, as indicated in Figure 3. The pressures of the other two low column density components, at 13.2 km s^{-1} and at 3.5 km s^{-1} , if indeed present, cannot be determined from the current data.

3.2. Interstellar S I

The species, S I, like C I, is preferentially formed in denser regions. However, S I is expected to have a behavior closer to that of C I than to those of Na I and K I. The ionization equilibria of C I and S I with ionization potential at 11.3 and 10.4 eV, respectively, are much more sensitive to $E(B-V)$ than are those of Na I (5.1 eV) and K I (4.3 eV). Thus, the distribution of S I is expected to track closely that of C I. The ratio of $N(\text{C I})/N(\text{S I})$ deduced here for the 6.0 km s^{-1} component, the only component in which it is definitely identified, is roughly 40, which is in good agreement with the work of Gomez-Gonzalez & Lequeux (1975) from whose analysis a value of 32 is derived for the same ratio using *Copernicus* data.

3.3. Molecular CO

Absorption from CO is seen at 1477 and 1447 Å, corresponding to the $A^1\Pi-X^1\Sigma^+$ system's 2-0 and 3-0, bands, respectively. The observed spectra recorded at an average resolving power $\lambda/\Delta\lambda = 86500$ show well-resolved rotational lines R(0), R(1), and Q(1) and *no* detectable absorption from rotational levels $J \geq 2$. This is the first time that CO ultraviolet lines from individual rotational levels have been resolved. Our estimates of the CO column density and excitation temperature were provided by fitting synthetic spectra to the observations. Basic ingredients for these synthetic spectra were accurate wavelengths (Brown 1991) and band oscillator strengths $f_{20} = 0.0412$ and $f_{30} = 0.0361$ estimated from radiative lifetimes of the $A^1\Pi$ state (Field et al. 1983; Le Floch, Rostas, & Rostas 1990; see van Dishoeck & Black 1987). We assumed that the CO is distributed among three distinct clouds seen in very high resolution spectra ($\lambda/\Delta\lambda = 500000$) of the CH 4300.3 Å line (Crane & Lambert 1991): the characteristics of the CH clouds are (6.9, 2.14, 0.42), (10.4, 2.3, 0.35), and (12.9, 10.9, 0.23), where the numbers in parentheses are, in order, the heliocentric radial velocity (in km s^{-1}), the b -value (in km s^{-1}) of the (assumed) Gaussian line profile, and the relative column density. Synthetic spectra were computed on the assumption that the CO and CH molecules were similarly distributed through the three clouds. Previous results (Federman & Lambert 1988) show that CO and CH are tightly correlated. (There is no evidence in the observed CH profiles for a fourth cloud at 3.5 km s^{-1} .)

The spectra in Figure 4, which provide an acceptable fit to the observations, correspond to a total column density $N(\text{CO}) = (3.1 \pm 0.3) \times 10^{13} \text{ cm}^{-2}$ and an excitation temperature $T_{\text{exc}} = 4.0 \pm 0.3 \text{ K}$, where a single T_{exc} was adopted for all clouds. It is likely that T_{exc} is different in the three clouds, but spectra of higher quality will be needed to establish that the differences parallel those inferred from the C I lines. The

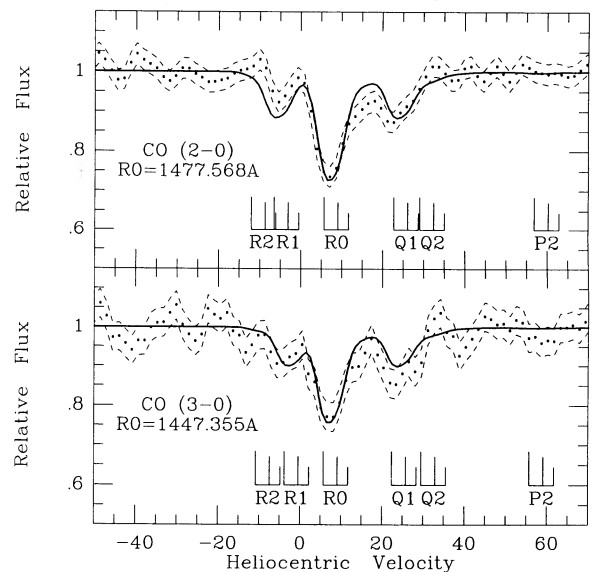


FIG. 4.—Normalized CO spectra of bands in the $A^1\Pi-X^1\Sigma^+$ system. *Dots*: observations. *Dashed lines*: $\pm 1 \sigma$ counting statistics uncertainty. *Solid lines*: synthetic spectra using contributions from three component clouds. *Short vertical lines*: velocities of component clouds with lengths proportional to relative CO abundance in each component, being in the ratio of 0.42/0.35/0.23.

synthetic and observed spectra match well in velocity, suggesting that CO/OH ratios of the three components are similar, as assumed. Note that the laboratory CO wavelengths are accurate to $\pm 0.4 \text{ km s}^{-1}$ (Brown 1991).

CO toward ξ Per was detected previously from *Copernicus* spectra of the $C^1\Sigma^+-X^1\Sigma^+$ system's 0-0 band at 1088 Å (Jenkins et al. 1973). Our reanalysis of the spectra gives $N(\text{CO}) = (3.9 \pm 0.5) \times 10^{13} \text{ cm}^{-2}$ and $T_{\text{exc}} \simeq 4 \text{ K}$ for an adopted f -value, $f_{00} = 0.089$ (van Dishoeck & Black 1986), and our three-cloud model. These results are consistent with our new results from the $A-X$ system's bands and the uncertainties in the theoretical and experimental estimates of the f -values.

Calculations of the CO rotational populations have been reported by Smith, Krishna Swamy, & Stecher (1978), Wannier, Penzias, & Jenkins (1982), and van Dishoeck & Black (1987). Our low inferred T_{exc} is matched by a range of physical conditions from low kinetic temperature and high gas ($\text{H} + \text{H}_2$) density to high kinetic temperature and low gas density: inspection of the above calculations suggest $nT \sim 5000 \text{ cm}^{-3} \text{ K}$ is required for $T_{\text{exc}} \sim 4 \text{ K}$. Since excitation of CO is probably dominated by $\text{H}_2 + \text{CO}$ rather than $\text{H} + \text{CO}$ collisions, we have $n(\text{H}_2)T \sim 5000 \text{ cm}^{-3} \text{ K}$. For similar clouds along the lines of sight to ζ Oph, ζ and o Per, van Dishoeck & Black (1986) estimate $20 \text{ K} \leq T \leq 40 \text{ K}$ from the rotational populations of H_2 and C_2 . If $T = 32 \text{ K}$, corre-

sponding to the $\log T = 1.5$ isotherm in Figure 3, $n(\text{H}_2) \sim 156 \text{ cm}^{-3}$, which is similar to densities found in the ζ Oph, ζ and o Per clouds.

The density of molecular hydrogen estimated here is approximately consistent with the pressure determined from the 6.0 km s^{-1} component in the C I spectra. If $P/k = 40,000 \text{ cm}^{-3} \text{ K}$, and the excitation of the C I fine-structure levels is due primarily to collisions with hydrogen atoms, then $n(\text{H}) = 1200 \text{ cm}^{-3}$. (Again, we assume $T = 32 \text{ K}$.) The ratio $n(\text{H}_2)/n(\text{H})$ becomes 0.12. The total uncertainty affecting $n(\text{H}_2)/n(\text{H})$ may be a factor of 2; for example. If the lower limit on P/k is used, the ratio of $n(\text{H}_2)/n(\text{H}) = 0.25$. Savage et al. (1977) give the ratio of the column densities as $N(\text{H}_2)/N(\text{H}) = 0.25$, which is in agreement with our derived lower limit value.

The efforts of many people at the STScI, Ball Aerospace System Group, BASG, and NASA have contributed to making the early observations with the GHRS successful. We especially wish to thank the OSS staff at the STScI and the BASG engineers, H. Garner, J. Troeltzsch, C. Peck, and J. Kinsey. We also thank C. M. Brown for providing accurate CO wavelengths and Tricia Meylan and Michelle Fitzerka for their assistance in preparing this paper. D. L. L. acknowledges support through NASA contract NAS 5-29410.

REFERENCES

- Brown, C. M. 1991, private communication
 Cardelli, J. A., et al. 1991, ApJ, 377, 57
 Crane, P. C., & Lambert, D. L. 1991, in preparation
 Federman, S. R., & Lambert, D. L. 1988, ApJ, 328, 777
 Field, R. W., Benoist d'Azy, O., Lavolee, M., Lopez-Delgado, R., & Tramer, A. 1983, J. Chem. Phys., 78(6), 2838
 Gomez-Gonzalez, J., & Lequeux, J. 1975, A&A, 38, 29
 Jenkins, E. B., & Shaya, E. J. 1979, ApJ, 231, 55
 Le Floch, A., Rostas, J., & Rostas, F. 1990, Chem. Phys., 142, 261
 Morton, D. C. 1991, ApJS, in press
 Savage, B. D., Bohlin, R. C., Drake, J. F., & Budich, W. 1977, ApJ, 216, 291
 Savage, B. D., et al. 1991, ApJ, 377, 53
 Savage, B. D., & Sembach, K. R. 1991, ApJ, in press
 Simmons, J. D., Bass, A. M., & Tilford, S. G. 1969, ApJ, 155, 345
 Smith, A. M., Krishna Swamy, K. S., & Stecher, T. P. 1978, ApJ, 220, 138
 van Dishoeck, E. F., & Black, J. H. 1986, ApJS, 62, 109
 ———. 1987, in Physical Processes in Interstellar Clouds, ed. G. Morfill & M. S. Scholer (Dordrecht: Reidel), 241
 Wannier, P. G., Penzias, A. A., & Jenkins, E. B. 1982, ApJ, 254, 100